DETECTION AND CHARACTERIZATION OF WATER-FILLED KARST CAVITIES USING ELECTRICAL RESISTIVITY TOMOGRAPHY (MANGALIA, ROMANIA)

Bogdan Mihai NICULESCU[1*], Maria Mădălina BUCUR[2*], Adrian TALMACIU[2], Cristina Mariana DRĂGHICI[2]

[1]University of Bucharest, Faculty of Geology and Geophysics, Department of Geological Engineering and Geophysics, 1 Nicolae Bălcescu Blvd., 010041 Bucharest, Romania

**e-mail: b.m.niculescu@gmail.com, bogdan.niculescu@unibuc.ro*

[2]University of Bucharest, Faculty of Geology and Geophysics, Doctoral School of Geology, 1 Nicolae Bălcescu Blvd., 010041 Bucharest, Romania

**e-mail: bucurmaria94@yahoo.com, maria-madalina.bucur@g.unibuc.ro*

DOI: 10.xxxx

Abstract. In recent years, Electrical Resistivity Tomography (ERT) surveys have been conducted in the northern and north-western areas of the port city of Mangalia (Romanian Black Sea coast), one of the main objectives being the imaging and characterization of the endokarst features developed in Sarmatian (Middle Miocene) limestones. We used an AGI SuperSting R8/IP resistivity meter with 64 electrodes, in dipole–dipole array configuration with 5 or 6 m electrode spacing. The apparent resistivity data were acquired along survey lines, oriented approximately north–south and east–west, located in the vicinity of the Mangalia Marsh protected natural area. On all survey lines, isolated low-resistivity anomalous zones with a relatively isometric shape were detected at depths between 12 and 30 m and interpreted as probable water-filled karst cavities developed within the limestones. In the western and northern areas of the Mangalia Marsh, resistivity values of 2.2–4.3 Ω·m estimated for the cavities infill, from the L1-norm inversion of dipole–dipole data, suggest slightly mineralized groundwater. In contrast, the lower resistivities of 0.6–1.2 Ω·m obtained for the infill of cavities detected east of the Marsh, along the Saturn–Venus coastal sector, may indicate brackish water, possibly reflecting seawater intrusion into the karst system. These preliminary results highlight the benefits of extending the study to a wider area around Mangalia, to improve the understanding of subsurface karst processes, groundwater circulation, the optimal placement of groundwater extraction boreholes, and the assessment of geotechnical hazards related to karstified carbonate terrains.

Key words: Electrical resistivity tomography (ERT), Resistivity inversion, Karst aquifer, Coastal karst, Karst cavities, Seawater intrusion, Groundwater salinity, Thermomineral groundwater, Sarmatian (Middle Miocene), Dipole–dipole array

1. INTRODUCTION

Karst environments are extremely heterogeneous hydrogeological systems resulting from the combined effects of fracturing, groundwater circulation, and the dissolution of carbonate formations. These processes can lead to significant and often unpredictable variations in the physical properties of rocks due to the uneven spatial distribution of pore space, permeability, and water content, associated with the presence of fractures, cavities (voids), and underground drainage channels. These characteristics limit the efficiency and applicability of direct subsurface investigation methods based on drillings and have led to the increasingly widespread use of indirect geophysical methods (Binley and Kemna, 2005; Reynolds, 2011; Cheng *et al.*, 2019a).

Geoelectrical methods, particularly the Electrical Resistivity Tomography (ERT), are among the most frequently used geophysical techniques for investigating karst environments, as they can provide high-resolution 2D or 3D images of the electrical resistivity distribution in the subsurface (Binley and Kemna, 2005; Reynolds, 2011;

Redhaounia *et al.*, 2016; Cheng *et al.*, 2019a, 2019b; Torrese, 2020; Loke, 2025; Negri and Barbolla, 2025). The identification of cavities, groundwater flow pathways, and tectonic discontinuities – fracture zones or faults – is based on the often significant resistivity contrast between these features and the surrounding carbonate host rocks.

The increasing applicability and efficiency of geoelectrical methods for hydrogeological, geotechnical, and environmental studies in karst terrains have been facilitated by technical and methodological advances, including improvements in multi-electrode acquisition systems and survey techniques, the development of algorithms and software applications for apparent resistivity data inversion (Loke and Dahlin, 2002; Loke *et al.*, 2003; Loke *et al.*, 2013; Loke, 2025), and their integration with other geophysical methods (*e.g.* seismics, Ground Penetrating Radar – GPR) (Torrese, 2020; Amanatidou *et al.*, 2022; May *et al.*, 2024; Zhang *et al.*, 2024; Negri and Barbolla, 2025).

Coastal karst areas may exhibit particular features from a geoelectrical perspective: karst cavities are frequently water-saturated, and the mixing of freshwater with seawater may increase their conductivity (i.e., decreased resistivity), thereby reducing the electrical contrast with adjacent conductive formations and sometimes masking the presence of these cavities. Some studies indicate that, under these conditions, the inversion of apparent resistivity data may overestimate the depth or dimensions of karst cavities. Therefore, numerical modelling, the integration of ERT with other geophysical investigation methods, and the calibration of quantitative interpretations using direct information (boreholes, hydrogeological data) are essential for the correct interpretation of ERT surveys (Redhaounia *et al.*, 2016; Amanatidou *et al.*, 2022; Negri and Barbolla, 2025).

In the southern sector of the Romanian Black Sea coast (Costinești and Vama Veche), geoelectrical investigations carried out over the period 1991–2019 using vertical electrical sounding (VES) and ERT methods have primarily aimed at the identification, mapping, and monitoring of areas affected by seawater intrusion (Niculescu, 2018a; Niculescu and Andrei, 2019; Niculescu, 2020; Niculescu and Andrei, 2021). Over the past few years, ERT surveys have also been conducted in the northern and north-western sectors of the port city of Mangalia (Romanian Black Sea coast), adjacent to the Mangalia Marsh protected natural area, one of the objectives being the imaging and characterization of the endokarst features developed in Middle Miocene (Sarmatian stage) limestones (Niculescu *et al.*, 2024a). The study site is of particular interest because it hosts both an extensive karst system and ascending sulfur-rich thermomineral groundwater springs, some of which are exploited and used for therapeutic purposes (Feru and Capotă, 1991; Constantinescu, 2002).

In this paper, we present new insights into the geoelectrical detection and analysis of water-filled karst cavities, based on ERT survey lines located at different distances from the sea coast. The results of this study may contribute to an improved hydrogeological characterization of the karst aquifer in Mangalia area, the assessment of its vulnerability, the identification of suitable locations for thermomineral groundwater extraction boreholes, as well as the evaluation of geotechnical hazards and the risks associated with this type of carbonate terrains.

2. GEOLOGICAL, TECTONIC AND HYDROGEOLOGICAL SETTING OF THE STUDY AREA

The Mangalia area, where our ERT survey was conducted, is located near the Romanian coast of the Black Sea, in the Southern Dobrogea region – a tectonic compartment belonging to the Moesian Platform. This unit is bounded by the Capidava–Ovidiu crustal fault to the north, by the Intra-Moesian crustal fault (and the Romanian–Bulgarian border) to the south, by the Danube Fault to the west, while to the east its boundary is conventionally defined by the Black Sea (Fig. 1).

The Precambrian crystalline basement of Southern Dobrogea is overlain by a sedimentary cover deposited unconformably in several sedimentary cycles reflecting alternating marine transgressions and exondations: Cambrian–Carboniferous, Permian–Triassic, Jurassic–Cretaceous, Eocene–Oligocene, and Miocene–Pliocene (Late Badenian–Romanian) (Săndulescu, 1984; Ionesi, 1994; Juravle, 2009; Mutihac and Mutihac, 2010). These are overlain by Quaternary continental deposits, composed of reddish clays and silty clays (Early Pleistocene), followed by loess with intercalated paleosols (Middle–Late Pleistocene), forming an almost continuous cover up to 40 m thick (Ionesi, 1994; Juravle, 2009; Mutihac and Mutihac, 2010).

Relevant to the present study are the deposits of the last sedimentary cycle, particularly those of the Sarmatian stage, which cover the entire Southern Dobrogea platform. These deposits were formed in a shallow-marine environment and include clays, marls, and sands, followed predominantly by oolitic and lumachellic limestones, locally interbedded with clayey–marly horizons and calcareous sandstones (Ionesi, 1994; Juravle, 2009; Mutihac and Mutihac, 2010). These limestones, which in the study area have an average thickness of about 100 m, host a karst system whose development was favored by the circulation of thermomineral groundwaters rich in H_2S (Feru and Capotă, 1991; Constantinescu, 1995; Lascu *et al.*, 1995; Constantinescu, 2002; Marin, 2010). The exokarst is represented mainly by dissolution and collapse dolines, but karstification is more evident in the subsurface, including large endokarst features such as Limanu and Movile caves (Constantinescu, 1995; Lascu *et al.*, 1995; Constantinescu and Constantin, 2001; Constantinescu, 2002).

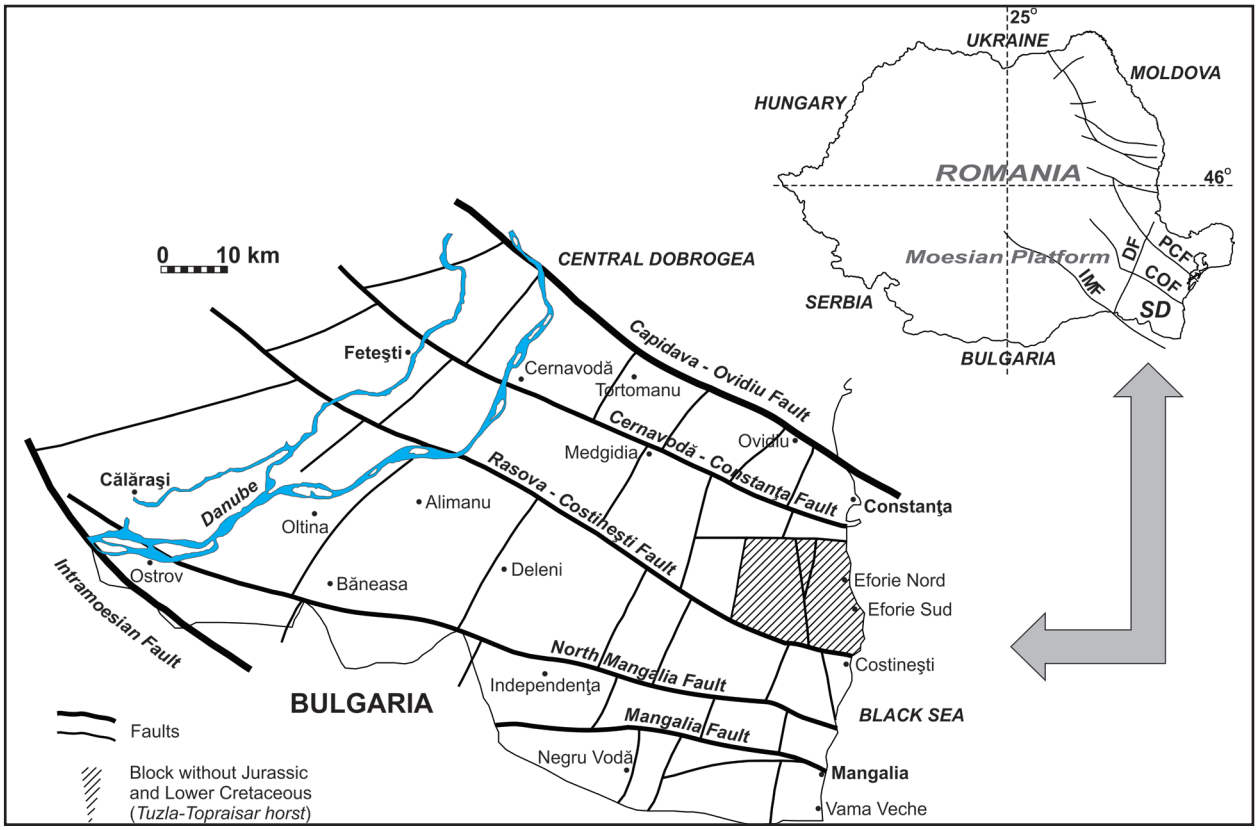

Fig. 1. Tectonic map of Southern Dobrogea (SD), with the location of the study area and the main fault systems. **IMF** – Intra-Moesian fault, **COF** – Capidava–Ovidiu fault, **PCF** – Peceneaga–Camena Fault, **DF** – Danube Fault (based on Moldoveanu, 1998; Dinu *et al.*, 2005; Niculescu and Andrei, 2019, 2021; Niculescu *et al.*, 2024b).

A prominent landform in the study area, located north of the port city of Mangalia, is the Mangalia Marsh, a coastal wetland/lake formed in a doline more than 1 km in diameter and fed by multiple ascending sulfurous thermomineral springs (Constantinescu, 1995; Lascu *et al.*, 1995; Constantinescu, 2002).

From a tectonic perspective, Southern Dobrogea is affected by two regional fault systems with general orientations NW–SE (or WNW–ESE) and NE–SW (or NNE–SSW) (Săndulescu, 1984; Visarion *et al.*, 1990; Dinu *et al.*, 2005). These faults have subdivided the platform into multiple blocks with variable thickness and different positions of stratigraphic boundaries (Fig. 1).

In this region, two superposed aquifers are present, both hosted in carbonate rocks (Țenu *et al.*, 1987; Feru and Capotă, 1991; Țenu *et al.*, 2002; Niculescu, 2018b; Niculescu *et al.*, 2024b). The lower aquifer (RODL06 transboundary groundwater body) is developed in fractured and karstified limestone and dolomites of Late Jurassic–Early Cretaceous age and is recharged mainly from the territory of Bulgaria, in the Pre-Balkan Plateau. The thickness of this complex decreases gradually from southwest to east and northeast, from more than 1000 m to about 400 m. Groundwater flow is mainly oriented along a SW–NE direction, occurring both through fractures and karst voids within the carbonate deposits and along fault planes. The upper aquifer (RODL04 transboundary groundwater body), hosted in the Sarmatian oolitic and lumachellic limestones, is predominantly unconfined, recharged mainly by precipitation, and exhibits a general west–east groundwater flow direction. This aquifer is overlain by Quaternary deposits, mainly permeable loess, and locally by the basal impermeable clay layers. The presence of sulfurous thermomineral springs in Mangalia area – including in the zones investigated in our ERT survey, which are adjacent to the Mangalia Marsh – appears to be primarily associated with the Sarmatian karstic aquifer (Ciocârdel and Protopopescu-Pache, 1955; Feru and Capotă, 1991).

3. GEOELECTRICAL DATA ACQUISITION AND PROCESSING METHODOLOGY

The ERT surveys carried out in recent years in the northern and north-western areas of the port city of Mangalia were conducted along lines with approximate north–south and east–west orientations, located adjacent to the Mangalia Marsh protected natural area (Figs. 2, 3, 4). Apparent resistivity (ρ_A) data were acquired using an AGI SuperSting R8/IP system (Advanced Geosciences, Inc.) equipped with 64 electrodes, in dipole–dipole array configuration (Binley and Kemna, 2005; Reynolds, 2011; Loke, 2025) with electrode spacings of 5 or 6 m.

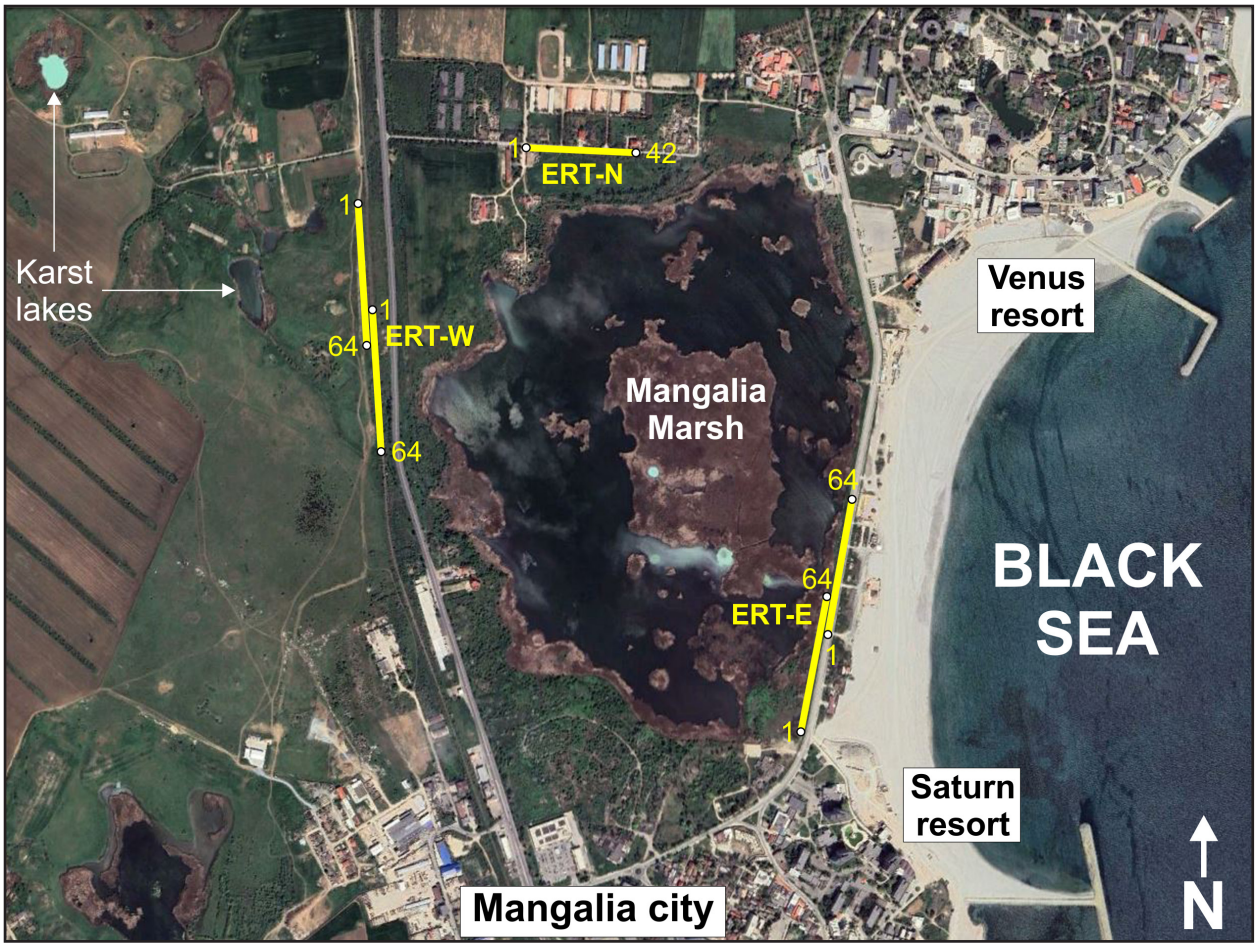

Fig. 2. Location of the ERT survey lines recorded in the vicinity of Mangalia Marsh protected natural area (north and northwest of the port city of Mangalia). The numbers (1, 42, 64) indicate the positions of the first and last electrodes of the deployed dipole–dipole arrays.

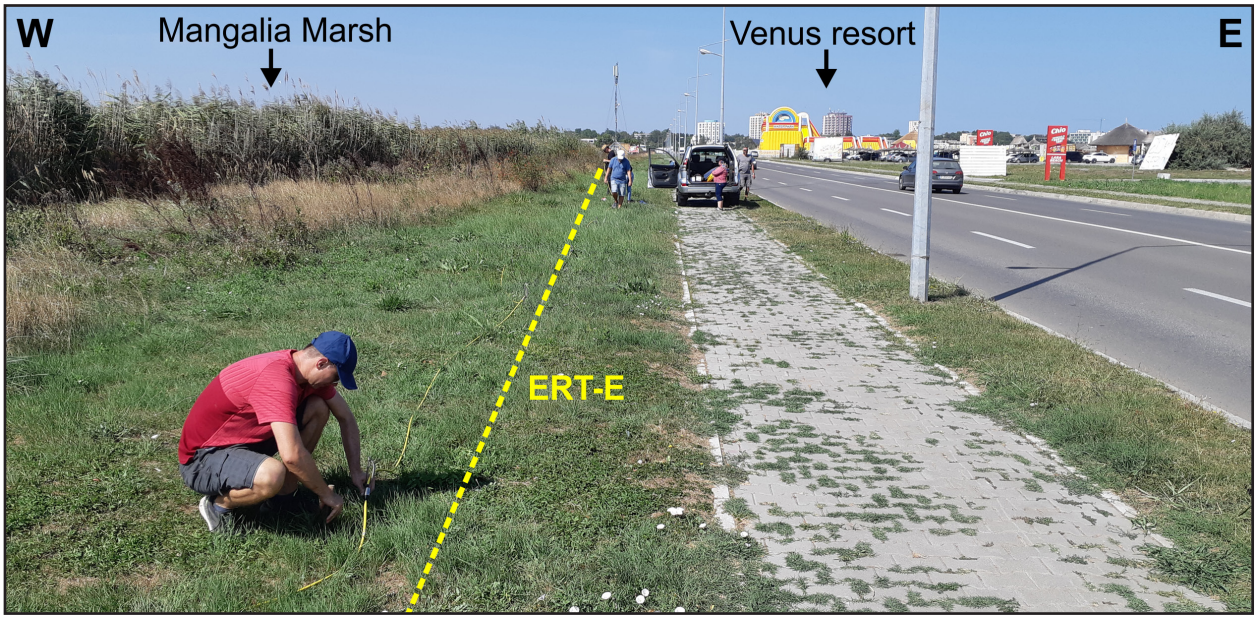

Fig. 3. Apparent resistivity data acquisition along survey line ERT-E.

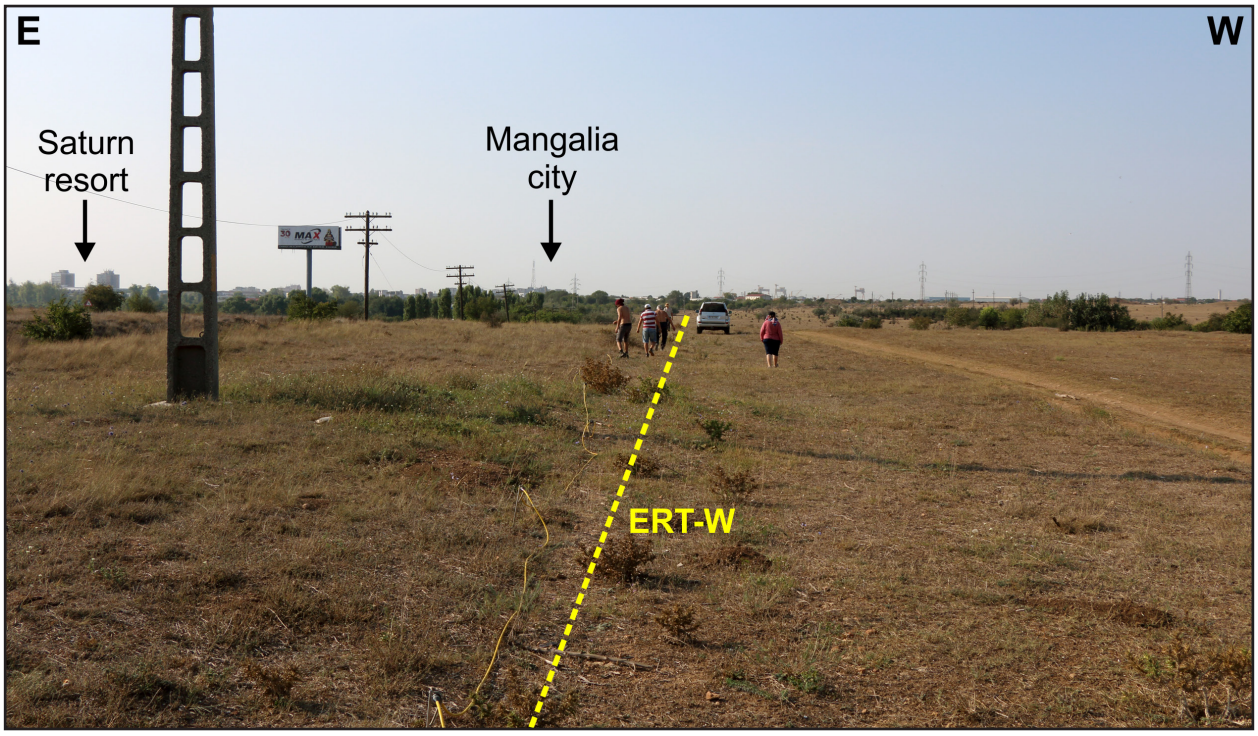

Fig. 4. Apparent resistivity data acquisition along survey line ERT-W.

The dipole–dipole array (Fig. 5) was employed due to its very fast multichannel acquisition capability and high sensitivity to horizontal resistivity variations (i.e., vertical subsurface features), making it particularly suitable for detailed imaging of fractured and/or complex geological structures, such as karst cavities. It also provides a larger number of data levels compared to other electrode configurations, resulting in denser and higher-resolution ρ_A datasets. The array consists of multiple combinations of current electrode pairs (C1, C2) and potential (measurement) electrode pairs (P1, P2), with the distance between them equal to or greater than the electrode spacing. The apparent resistivity of the subsurface can be expressed as:

$$\rho_A = \pi\, a\, n\, (n+1)\, (n+2)\, \frac{\Delta V}{I}$$

where a is the electrode spacing, n is an integer multiplier (separation factor), ΔV is the potential (voltage) difference measured between the P1 and P2 electrodes, and I is the intensity of the current injected through the C1 and C2 electrodes (Loke, 2025).

For the purpose of this study, three representative ERT survey lines are presented and analyzed:

- **Line ERT-W** (555 m long), located west of Mangalia Marsh (near the European route E87 and the Constanța–Mangalia railway), has an approximate north–south orientation and lies 1.4–1.5 km from the Black Sea shoreline.

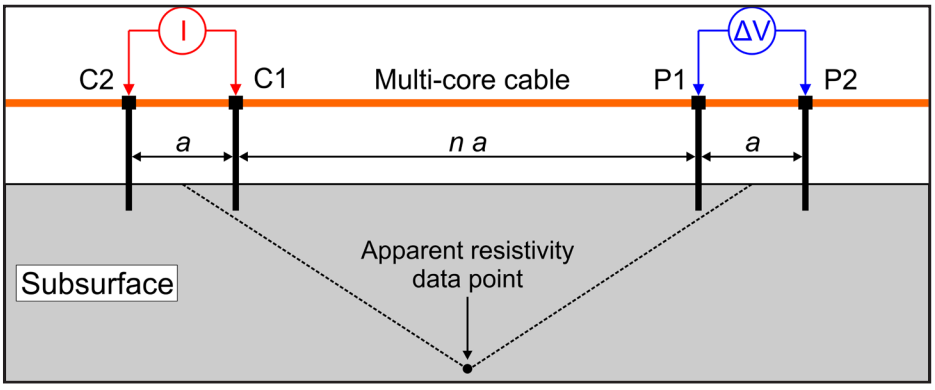

Fig. 5. Electrode arrangement and spacings for a dipole-dipole ERT array. **C1**, **C2** – current electrodes; **P1**, **P2** – potential (measurement) electrodes; a – electrode spacing; n – dipole separation factor; I – injected current; ΔV – measured potential (voltage) difference. The reference point for the measured apparent resistivity values is also indicated, being located at the midpoint between the two dipoles (electrode pairs) and at a conventional pseudo-depth corresponding to half the distance between their centers.

Measurements were carried out using two 64-electrode spreads at 5 m spacing, including a central overlap of 16 electrodes;

- **Line ERT-N** (246 m long), located north of Mangalia Marsh, is oriented approximately east–west and situated at an average distance of ~1 km from the shoreline. Data were collected using a single spread of 42 electrodes with 6 m spacing;
- **Line ERT-E** (555 m long), positioned along the eastern margin of Mangalia Marsh (Saturn–Venus beach sector), has an approximate north–south orientation and is located 250–300 m from the shoreline. Measurements were conducted using two 64-electrode spreads at 5 m spacing, with a 16-electrode overlap in the central section.

The inversion of the ρ_A datasets to obtain 2D geoelectrical models of the subsurface was carried out using the RES2DINV software (Loke, 2010, 2025). The applied method was the L1-norm robust (blocky) inversion, which optimizes an initial true resistivity model through the iterative minimization of the misfit between the measured ρ_A data and the model's theoretical response. The iterative optimization process stops when a user-defined acceptable minimum data misfit is reached or when the misfit can no longer be significantly reduced.

The resulting 2D interpretation models, which discretize the subsurface, consist of a large number of rectangular blocks (cells) with different true resistivity values. In the case of robust inversion of the ρ_A data, these models tend to display sharp boundaries, allowing a better approximation of geological features such as fractures or cavities. Forward modeling of the models' theoretical response was performed using the finite-difference algorithm incorporated in RES2DINV software. The finest mesh option, with four nodes per electrode spacing, was used, and the effect of the model's boundary blocks was slightly reduced to limit inversion artifacts.

4. RESULTS AND DISCUSSION

Figures 6–9 show the geoelectrical models (true resistivity sections) obtained from the L1-norm inversion of dipole–dipole ρ_A data for the three survey lines analyzed in this study.

In general, the Sarmatian limestones are well imaged and are characterized by high to very high resistivity values, contrasting with the overlying Quaternary formations, which are more conductive.

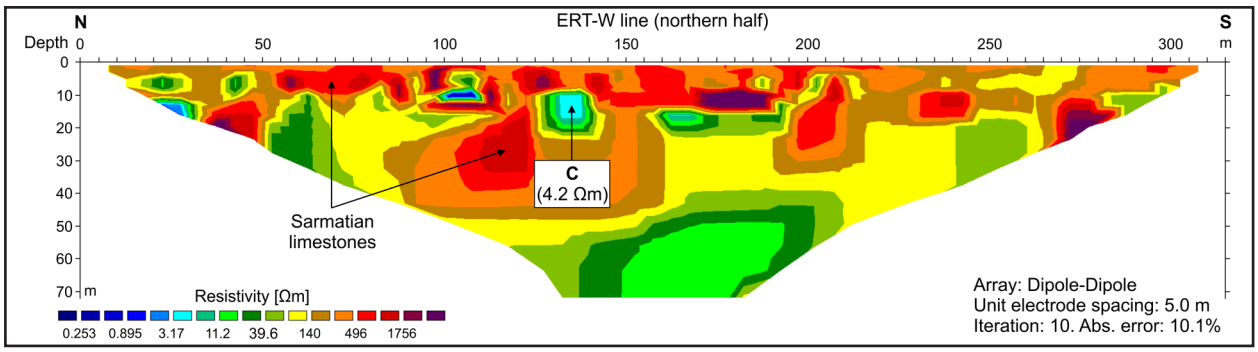

Fig. 6a. Geoelectrical model (true resistivity section) derived from the L1-norm inversion of dipole–dipole ρ_A data for the ERT-W survey line, first 64-electrode spread (northern half of the line). *x*-axis: distance along the line; *z*-axis: depth; datum points: 1918; data levels: 48; line length: 315 m. **C** – probable water-filled karst cavity, with the calculated resistivity of the cavity infill indicated.

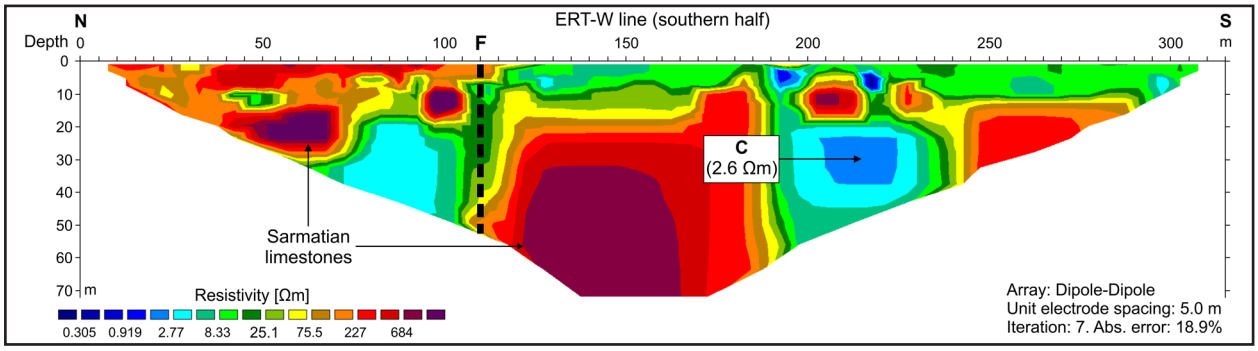

Fig. 6b. Geoelectrical model (true resistivity section) derived from the L1-norm inversion of dipole–dipole ρ_A data for the ERT-W survey line, second 64-electrode spread (southern half of the line). *x*-axis: distance along the line; *z*-axis: depth; datum points: 1789; data levels: 48; line length: 315 m. **F** – interpreted fault; **C** – probable water-filled karst cavity, with the calculated resistivity of the cavity infill indicated.

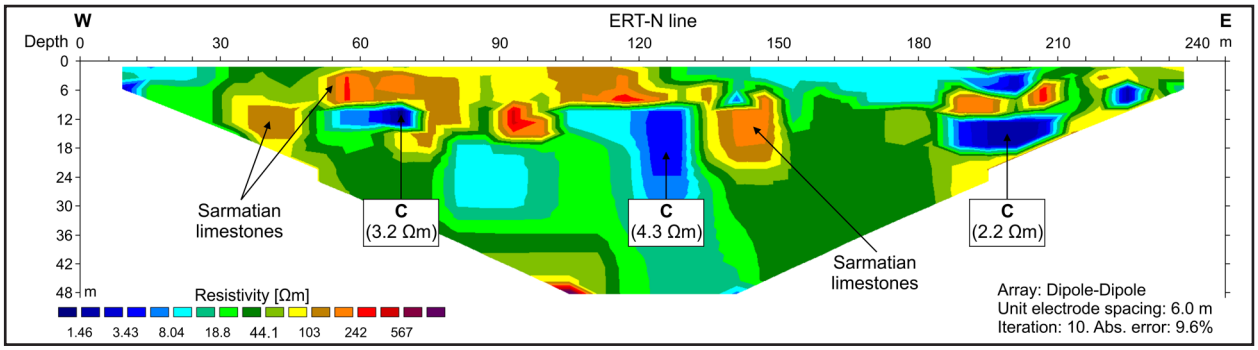

Fig. 7. Geoelectrical model (true resistivity section) derived from the L1-norm inversion of dipole–dipole ρ_A data for the ERT-N survey line, 42-electrode spread. *x*-axis: distance along the line; *z*-axis: depth; datum points: 946; data levels: 40; line length: 246 m. **C** – probable water-filled karst cavities, with the calculated resistivity of the cavities infill indicated.

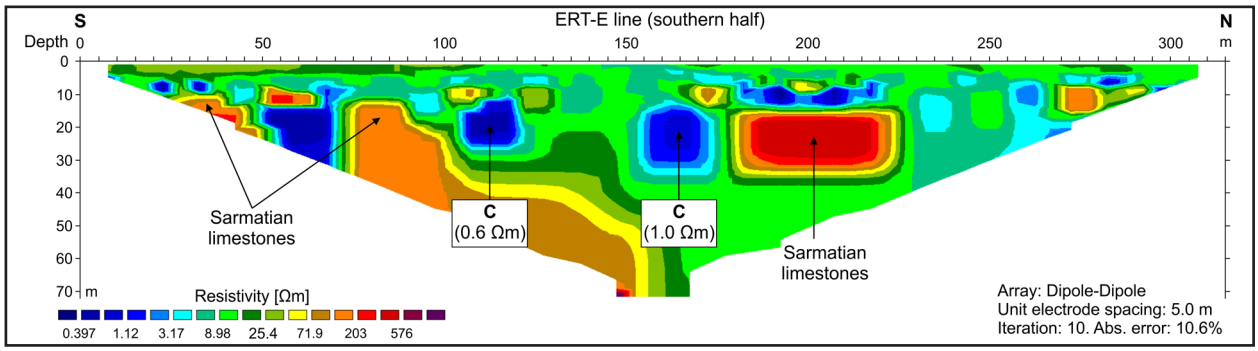

Fig. 8a. Geoelectrical model (true resistivity section) derived from the L1-norm inversion of dipole–dipole ρ_A data for the ERT-E survey line, first 64-electrode spread (southern half of the line). *x*-axis: distance along the line; *z*-axis: depth; datum points: 1955; data levels: 48; line length: 315 m. **C** – probable water-filled karst cavities, with the calculated resistivity of the cavities infill indicated.

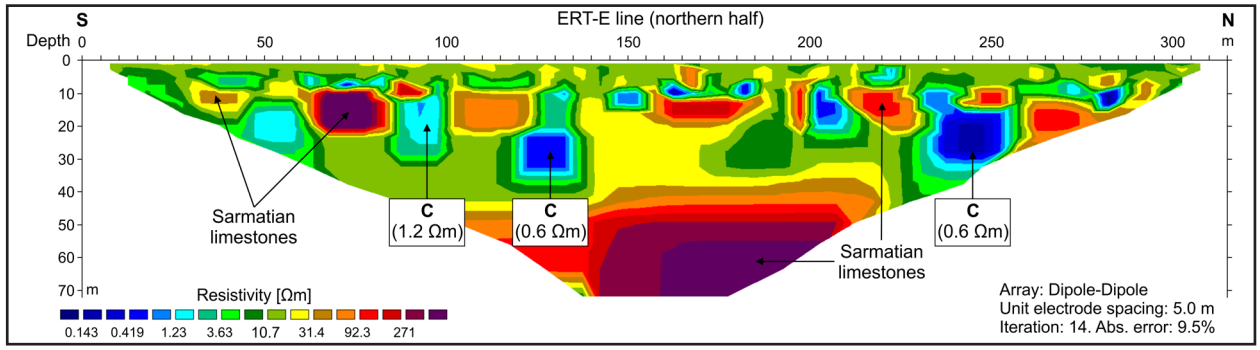

Fig. 8b. Geoelectrical model (true resistivity section) derived from the L1-norm inversion of dipole–dipole ρ_A data for the ERT-E survey line, second 64-electrode spread (northern half of the line). *x*-axis: distance along the line; *z*-axis: depth; datum points: 1935; data levels: 48; line length: 315 m. **C** – probable water-filled karst cavities, with the calculated resistivity of the cavities infill indicated.

However, the resistivity of the limestones varies significantly along the three survey lines, ranging from more than 100 Ω·m to several thousand Ω·m in the most compact zones, particularly along the ERT-W line. Along some portions of the survey lines, where it could be more clearly delineated, the top of the limestones appears to be located at depths of 8–12 m (possibly with local variations down to 12–14 m on the ERT-E line), while it is more difficult to delineate on the ERT-N line. On the ERT-W line, along the first electrode spread (Fig. 6a) and in the first third of the second electrode spread (Fig. 6b), the top of the Sarmatian limestones is imaged very close to the surface, unlike its position along the remaining part of the line, where it appears downthrown. This lateral change may indicate the presence of a fault intersecting the line, likely between 100–120 m of the second electrode spread.

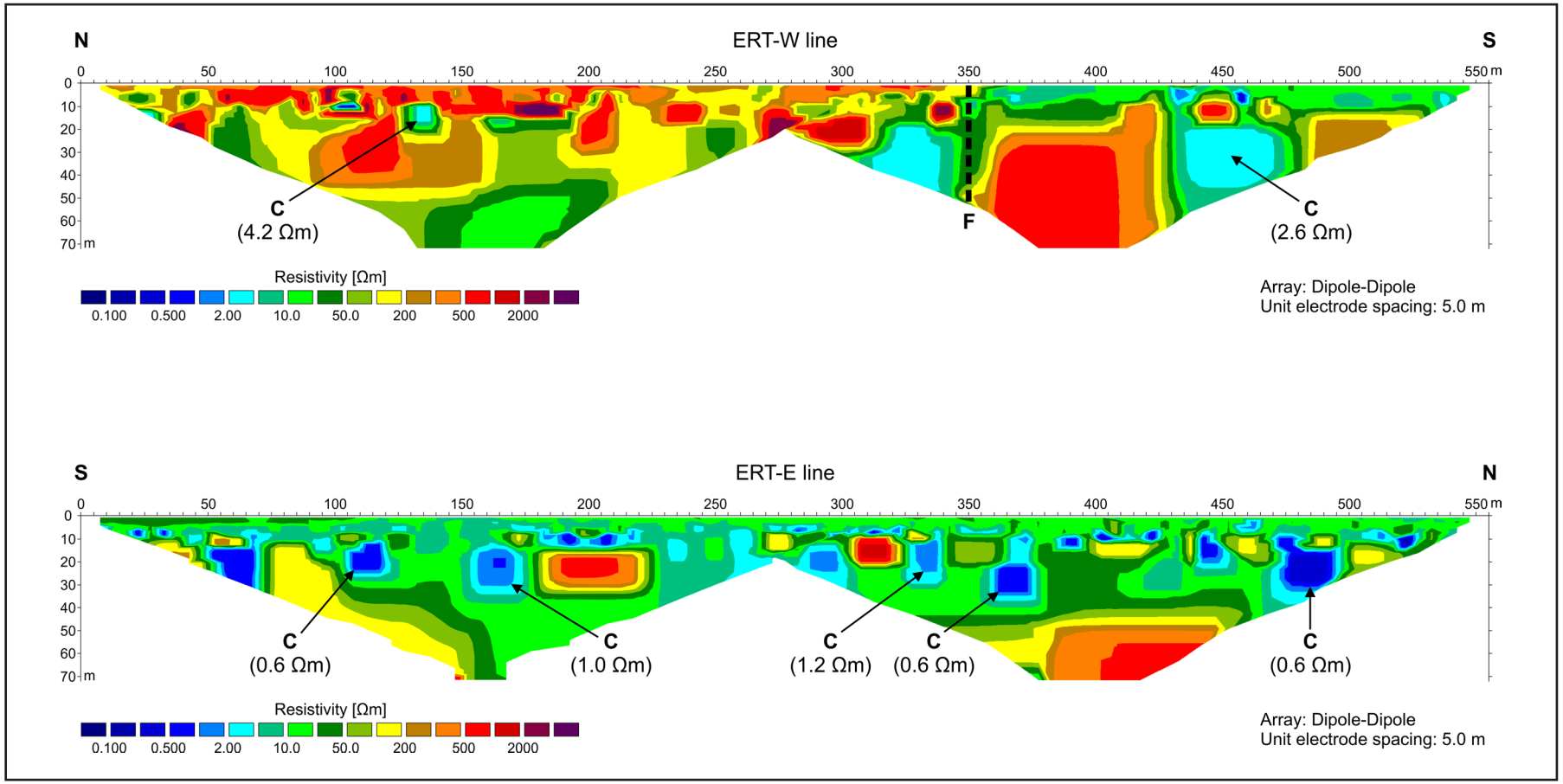

Fig. 9. Geoelectrical models (true resistivity sections) derived from the L1-norm inversion of dipole–dipole ρ_A data for the complete ERT-W and ERT-E survey lines, merged at the central overlap of the cable spreads. *x*-axis: distance along the lines; *z*-axis: depth. **F** – interpreted fault; **C** – probable water-filled karst cavity, with the calculated resistivity of the cavity infill indicated.

On all survey lines, isolated low-resistivity anomalous zones with a relatively isometric shape were detected at depths between 12 and 30 m and interpreted as probable water-filled karst cavities developed within the limestones. Some of these anomalies (*e.g.*, on the second electrode spread of the ERT-W line between 205–225 m, or on the ERT-N line between 122–130 m) could also be interpreted as the terminations of subvertical fracture zones through which groundwater circulates.

The actual dimensions of the karst cavities are difficult to determine accurately. Their apparent horizontal and vertical extents estimated from inverted geoelectrical models depend on the electrode spacing used and the size of rectangular blocks employed by the RES2DINV software to discretize the subsurface. Therefore, these apparent extents may substantially overestimate the true size of the cavities.

The inverted ERT sections shown in Figs. 6–9 allowed the estimation of water resistivity (ρ_w) and, implicitly, of the equivalent NaCl salt concentration/salinity (c_w) for the waters filling the likely karst cavities. Table 1 presents the results of this estimation for the cavities detected along the survey lines, with their positions indicated by the coordinates of their centers (x_c , z_c). The estimation of c_w was based on its dependence on ρ_w and temperature (Schlumberger, 2013), with values referenced to a standard temperature of 20 °C. It is important to note that the most representative values of ρ_w were taken as the minimum resistivity values calculated from the inversion algorithm at the centers of the detected low-resistivity anomalous zones. This implies that the c_w values listed in Table 1 represent maximum salt concentrations, while the actual concentrations may be lower. It should also be noted that the c_w values estimated using a NaCl reference may deviate, to varying degrees, from the actual salinity of the waters within the karst cavities if their chemical composition differs.

Regarding the thermomineral groundwaters hosted in the Sarmatian aquifer in Mangalia area, chemical analyses of samples collected from hydrogeological boreholes indicate that the waters are sulfurous, predominantly sodium chloride–type, bicarbonate (calcium–magnesium), with low bromine and iodine contents, and a total mineralization not exceeding 1.5 g/l (Feru and Capotă, 1991). In the western and northern areas of the Mangalia Marsh (ERT-W and ERT-N survey lines), the minimum ρ_w values estimated for the cavities infill range between 2.2 and 4.3 Ω·m, corresponding to c_w values of about 1.3–2.6 g/l (1320–2600 ppm) NaCl equivalent, and suggest slightly mineralized groundwater. This estimated c_w range is close to or slightly higher than the maximum total mineralization reported for borehole samples. In contrast, the significantly lower ρ_w values of 0.6–1.2 Ω·m obtained for the infill of cavities detected east of the Marsh (ERT-E survey line), along the Saturn–Venus coastal sector, may indicate brackish water with c_w of about 5–10 g/l (4930–10310 ppm) NaCl equivalent, possibly reflecting seawater intrusion into the karst system.

Table 1. Estimation of water parameters within the inferred karst cavities based on inverted ERT resistivity sections.

Survey line	x_c [m]	z_c [m]	ρ_w [Ω·m]	c_w [ppm NaCl] @ 20 °C
ERT-W (1st electrode spread)	135	14	4.2	1320
ERT-W (2nd electrode spread)	215	30	2.6	2180
ERT-N	66	12	3.2	1750
	125	17	4.3	1280
	199	15	2.2	2600
ERT-E (1st electrode spread)	113	19	0.6	10310
	164	23	1.00	5980
ERT-E (2nd electrode spread)	93	18	1.2	4930
	128	28	0.6	10310
	244	23	0.6	10310

x_c, z_c – position of the karst cavities center; ρ_w – resistivity of cavity-filling water; c_w – equivalent NaCl concentration (salinity) of the cavity-filling water at a standard temperature of 20°C.

5. CONCLUSIONS

This study primarily aimed to test the applicability and effectiveness of modern geoelectrical investigation methods (ERT) for detecting karst cavities developed in Sarmatian limestones in the northern–northwestern part of the port city of Mangalia, located on the Romanian Black Sea coast. The ERT survey, carried out using a dipole–dipole array along three lines in the vicinity of the Mangalia Marsh protected area, successfully identified multiple electrically conductive anomalies with a relatively isometric geometry, occurring at variable depths and interpreted as likely water-filled karst cavities.

Estimates of the resistivity and salinity of the water filling these inferred cavities revealed significant variability as a function of distance from the coastline. For two of the survey lines located inland (ERT-W and ERT-N), at distances ≥1 km from the coastline, the estimated salinity values suggest slightly mineralized groundwater. These values are consistent with those obtained from chemical analyses of water samples collected from hydrogeological boreholes in the study area. However, along one survey line (ERT-E) located east of the Mangalia Marsh, the estimated salinity values for karst cavities infill are significantly higher, corresponding to brackish groundwater. This result suggests a seawater intrusion phenomenon, likely facilitated by the presence of karst conduits and a fracture network within the Sarmatian limestones.

To our knowledge, this is the first systematic ERT study dedicated to the detection and characterization of karst cavities in the northern–northwestern Mangalia area and also the first to suggest a possible marine influence affecting the coastal Sarmatian aquifer, at least up to distances of approximately 250–300 m from the Black Sea coastline. The preliminary results obtained highlight the benefits of extending this geoelectrical investigation to a wider area around Mangalia in order to improve the understanding of subsurface karst processes, groundwater circulation, and the assessment of geotechnical hazards associated with karstified carbonate terrains. Another practical application of this study concerns the optimal placement of future boreholes for the exploitation of thermomineral groundwater, intercepting karst cavities through which it circulates.

A limitation of this ERT study is related to the use of a single electrode configuration, namely the dipole–dipole array. Therefore, it is important to emphasize that the preliminary results presented – regarding the location and depth of the detected low-resistivity isometric anomalies, as well as the estimated resistivity and salinity values of the groundwater filling these probable karst cavities – are strictly representative of this array type. Accordingly, a future research direction involves the inclusion, analysis, and interpretation of apparent resistivity data obtained using additional electrode configurations (*e.g.*, Schlumberger and/or Wenner arrays), both along the three survey lines presented and along supplementary lines, in order to ensure better coverage of the study area using geoelectrical imaging data. This approach would allow the verification and extension of the results obtained using the dipole–dipole array and may lead to a more comprehensive characterization of the karst system developed in the Sarmatian limestones of Mangalia area.

REFERENCES

Amanatidou, E., Vargemezis, G., Tsourlos P. (2022). Combined application of seismic and electrical geophysical methods for karst cavities detection: A case study at the campus of the new University of Western Macedonia, Kozani, Greece. *Journal of Applied Geophysics*, **196**: 104499. https://doi.org/10.1016/j.jappgeo.2021.104499

Binley, A., Kemna, A. (2005). DC Resistivity and Induced Polarization Methods. *In*: Rubin, Y., Hubbard, S.S. (Eds.), *Hydrogeophysics*, Chapter 5: 129-156. Springer, Dordrecht, The Netherlands.

Cheng, Q., Chen, X., Tao, M., Binley, A. (2019a). Characterization of karst structures using quasi-3D electrical resistivity tomography. *Environ. Earth Sci.*, **78**: 285. https://doi.org/10.1007/s12665-019-8284-2

Cheng, Q., Tao, M., Chen, X., Binley, A. (2019b). Evaluation of electrical resistivity tomography (ERT) for mapping the soil–rock interface in karstic environments. *Environ. Earth Sci.*, **78**: 439. https://doi.org/10.1007/s12665-019-8440-8

Ciocârdel, R., Protopopescu-Pache, E. (1955). Considerații hidrogeologice asupra Dobrogei [Hydrogeological considerations on Dobrogea]. *Comitetul Geologic*, *Studii Tehnice și Economice*, *Seria E (Hidrogeologie)*, **3**: 3-51, București.

Constantinescu, T. (1995). Le karst de type Movile (Mangalia, Dobrogea de Sud, Roumanie). *Theoretical and Applied Karstology*, **8**: 91-96, București.

Constantinescu, T., Constantin, S. (2001). La genese et l'evolution des grandes dolines (obans) de la zone karstique de Mangalia (Dobroudja du Sud, Roumanie). *Theoretical and Applied Karstology*, **13**–**14** (2000-2001): 87–92, București.

Constantinescu, T. (2002). Le karst de la zone Mangalia. *Travaux de l`Institut de Spéologie „Émile Racovitza"*, **XLI–XLII** (2002–2003): 89-109, București.

Dinu, C., Wong, H.K., Țambrea, D., Mațenco, L. (2005). Stratigraphic and structural characteristics of the Romanian Black Sea shelf. *Tectonophysics*, **410**: 417-435. https://doi.org/10.1016/j.tecto.2005.04.012

Feru, M., Capotă, A. (1991). Les eaux thermominérales karstiques de la zone Mangalia (Roumanie). *Theoretical and Applied Karstology*, **4**: 143-157, București.

Ionesi, L. (1994). *Geologia unităților de platformă și a orogenului Nord-Dobrogean* [Geology of the platform units and the North Dobrogea Orogen]. Editura Tehnică, București, ISBN 973-31-0531-7.

Juravle, D.T. (2009). *Geologia României*, Volumul I, Geologia terenurilor Est-Carpatice (Platformele şi Orogenul Nord-Dobrogean) [Geology of Romania, Volume I: Geology of the East-Carpathian Terranes (Platforms and the North Dobrogean Orogen)]. Editura Stef, Iași, ISBN 978-973-1809-55-7.

Lascu, C., Popa, R., Sârbu, S. (1995). Le karst de Movile (Dobrogea de Sud) (I). *Revue Roum. Geogr.*, **38**: 86-93.

Loke, M.H., Dahlin, T. (2002). A comparison of the Gauss–Newton and quasi-Newton methods in resistivity imaging inversion. *Journal of Applied Geophysics*, **49**(*3*): 149-162. https://doi.org/10.1016/S0926-9851(01)00106-9

Loke, M. H., Acworth, I., Dahlin, T. (2003). A comparison of smooth and blocky inversion methods in 2D electrical imaging surveys. *Exploration Geophysics*, **34**(*3*): 182-187. https://doi.org/10.1071/EG03182

Loke, M.H. (2010). *RES2DINV ver. 3.59*, Rapid 2-D Resistivity & IP Inversion Using the Least-Squares Method. Geotomo Software, Gelugor, Penang, Malaysia.

Loke, M.H., Chambers, J.E., Rucker, D.F., Kuras, O., Wilkinson, P.B. (2013). Recent developments in the direct-current geoelectrical imaging method. *Journal of Applied Geophysics*, **95**: 135-156. https://doi.org/10.1016/j.jappgeo.2013.02.017

Loke, M.H. (2025). *Tutorial: 2-D and 3-D electrical imaging surveys*. Geotomo Software, Gelugor, Penang, Malaysia.

Marin, C., 2010. Geochemistry of the sulfide meso-thermal groundwater complex at Mangalia. *In*: Orășeanu, I., Iurkiewicz, A. (Eds.), *Karst hydrogeology of Romania*: 387-399. Belvedere Publishing House, Oradea, Romania.

May, M.T., Brackman, T.B., May, E.C., Edwards, W.T. (2024). Use of electrical resistivity tomography to reduce landfill siting risks in the south-central Kentucky karst. *Environ. Earth Sci.*, **83**: 688. https://doi.org/10.1007/s12665-024-11984-6

Moldoveanu, V. (1998). *Studiul condiţiilor hidrogeologice ale Dobrogei de Sud pentru reevaluarea resurselor exploatabile* [Study of the hydrogeological conditions of Southern Dobrogea for the reassessment of exploitable resources]. Ph.D. thesis, University of Bucharest, 164 p.

Mutihac, V., Mutihac, G. (2010). *The Geology of Romania within the Central-Est-European Geostructural Context*. Editura Didactică și Pedagogică, București, ISBN 978-973-30-2686-0.

Negri, S., Barbolla, D. F. (2025). Challenges in the Detection of Water-Filled Cavities in Karst Environments Using Electrical Resistivity Tomography. *Geosciences*, **15**(*9*): 349. https://doi.org/10.3390/geosciences15090349

Niculescu, B.M. (2018a). Forward Modeling of Vertical Electrical Soundings with Applications in the Study of Sea Water Intrusions. 18th International Multidisciplinary Scientific GeoConference SGEM 2018, Albena, Bulgaria, *Conference Proceedings*, **18**(*1.1*): 803-810. doi:10.5593/sgem2018/1.1/S05.101.

Niculescu, B.M. (2018b). Geophysical and Geological Investigations of the Late Jurassic–Early Cretaceous Aquifer in Cernavodă Area, South Dobrogea (Romania). 18th International Multidisciplinary Scientific GeoConference SGEM 2018, Albena, Bulgaria, *Conference Proceedings*, **18**(*1.1*): 825-832. doi:10.5593/sgem2018/1.1/S05.103.

Niculescu, B.M., Andrei, G. (2019). Using Vertical Electrical Soundings to Characterize Seawater Intrusions in the Southern Area of Romanian Black Sea Coastline. *Acta Geophysica*, **67**(*6*): 1845-1863. doi:10.1007/s11600-019-00341-y.

Niculescu, B.M. (2020). An Overview of Geoelectrical Surveys for the Assessment of Seawater Intrusion from the Romanian Black Sea Coastal Area. 20th Anniversary International Multidisciplinary Scientific GeoConference SGEM 2020, Albena, Bulgaria, *Conference Proceedings*, **20**(*1.2*): 427-434. doi:10.5593/sgem2020/1.2/s05.055.

Niculescu, B.M., Andrei, G. (2021). Application of electrical resistivity tomography for imaging seawater intrusion in a coastal aquifer. *Acta Geophysica*, **69**(*2*): 613-630. doi:10.1007/s11600-020-00529-7.

Niculescu, B.M., Talmaciu, A., Bucur, M.M. (2024a). Assessing the Effectiveness of Electrical Resistivity Tomography for Subsurface Investigation in a Seashore Karst Setting. *Mediterranean Geosciences Union 4th Annual Meeting* (MedGU-24), Barcelona, Spain, Paper #27. https://2024.program.medgu.org/#/program

Niculescu, B.M., Bucur, M.M., Talmaciu, A. (2024b). Groundwater Exploration in Carbonate Reservoirs Using Borehole Investigations: A Case Study from South Dobrogea, Romania. *Energies*, **17**(*2*): 426. doi:10.3390/en17020426.

Redhaounia, B., Ilondo, B.O., Gabtni, H., Sami, K. (2016). Electrical Resistivity Tomography (ERT) Applied to Karst Carbonate Aquifers: Case Study from Amdoun, Northwestern Tunisia. *Pure Appl. Geophys.* **173**: 1289-1303. https://doi.org/10.1007/s00024-015-1173-z

Reynolds, J.M. (2011). *An Introduction to Applied and Environmental Geophysics*, 2nd Edition. Wiley-Blackwell, ISBN 978-0-471-48535-3, 978-0-471-485360.

Schlumberger (2013). *Log Interpretation Charts*, 2013 Edition. SCHLUMBERGER Limited, Houston, TX, 306 p., ISBN 978-1-937949-10-5.

Săndulescu, M. (1984). *Geotectonica României* [Geotectonics of Romania]. Editura Tehnică, București.

Torrese, P. (2020). Investigating karst aquifers: Using pseudo 3-D electrical resistivity tomography to identify major karst features. *Journal of Hydrology*, **580**: 124257. https://doi.org/10.1016/j.jhydrol.2019.124257

Țenu, A., Davidescu, F.D., Slăvescu, A. (1987). Recherches isotopiques sur les eaux souterraines des formations calcaires dans la Dobroudja meridionale (Roumanie). *In: Isotope Techniques in Water Resources Development*, Internat. Atomic Energy Agency, Vienna: 439-453.

Țenu, A., Davidescu, F., Petres, R., Coarnă, L. (2002). Environmental isotopes studies and the hydrogeological model of South Dobrogea (Romania). *Theoretical and Applied Karstology*, **15**: 61-72, București.

Visarion, M., Săndulescu, M., Roșca, V., Stănică, D., Atanasiu, L. (1990). La Dobrogea dans le cadre de l'avant-pays carpatique. *Rev. Roum. Geophys.*, **34**: 55-65, București.

Zhang, J., Sirieix, C., Genty, D., Salmon, F., Verdet, C., Mateo, S., Xu, S., Bujan, S., Devaux, L., Larcanché, M. (2024). Imaging hydrological dynamics in karst unsaturated zones by time-lapse electrical resistivity tomography. *Science of the Total Environment*, **907**: 168037. https://doi.org/10.1016/j.scitotenv.2023.168037